Thermal Conductivity Calculated via Iterative Methods
APC 523 Final Project

Jiayi Hu

May 8, 2024

1 Introduction to the Problem

1.1 Thermal Conductivity

Thermal conductivity has always been an important technique while studying material properties. For metals, electrons are the major carriers for the heat and charges, leading to the Wiedemann-Franz law about thermal and electrical conductivity: $\kappa/\sigma = L\,T$, where T is the temperature and L is a constant. Hence, deviation from this ratio often signals some intriguing physics is at play. For insulators where electrical measurements are no longer applicable, thermal transport naturally a crucial tool people use to understand the system. While the major heat carrier is phonon, thermal conduction can also comes from magnons in magnetic materials, and other more exotic quasiparticles. One famous example in condensed matter physics is the quantum spin liquid. Despite its theoretical significance and various models, its experimental realization has been challenging due to lack of measurable observables. The decisive, if not only, smoking gun evidence of one of its models is a half-integer quantized signal in transverse thermal conductivity caused by majoranas, which attracts lots of interests recently[3][9][1]. Besides exploring the frontier of physics, thermal conduction also tights closely to daily life. Both good thermal conductors and good insulators are indispensable in many fields like microelectronics and aerospace.

1.2 Boltzmann Transport Equation

Given the importance of thermal conductivity, people have been working on methods to understand it, and even predict it. One of the widely used analysis that focuses on phonon conduction stems from the Boltzmann transport equation (BTE), which has the general form

$$\frac{df}{dt} = \left.\frac{\partial f}{\partial t}\right|_{\text{force}} + \left.\frac{\partial f}{\partial t}\right|_{\text{diff}} + \left.\frac{\partial f}{\partial t}\right|_{\text{sctt}} \tag{1}$$

. In the above equation, f is the density distribution, the terms on the right hand side are parts of its change caused by external force, diffusion, and scattering, respectively [[2]]. If we concerns the simplest transport experiment where a temperature gradient is applied and the system reachs steady state, we have a vanishing left hand side $\frac{df}{dt} = 0$ and the first term on the right. Therefore, writing out the change in f caused by diffusion gives

$$\left.\frac{\partial f}{\partial t}\right|_{diff} = -\vec{v}\cdot\vec{\nabla}T\frac{\partial f}{\partial T} = -\left.\frac{\partial f}{\partial t}\right|_{\text{sctt}} \tag{2}$$

1.3 RTA and Linearized BTE

At equilibrium state without any temperature gradient, phonon population is described by Bose-Einstein distribution

$$f_0(\omega_\lambda) = \frac{1}{\exp^{\hbar\omega_\lambda/k_BT} - 1}$$

, where λ denotes a shorthand index that includes wavevector $\vec{q}$ and phonon branch p.

Yet the right hand side is not as easy to address. It's been challenging to determine the scattering mechanisms and their mathematical forms. The prominent ones in just normal insulators are believed to include phonon-phonon Umklapp scattering (U process), phonon-phonon N scattering (discussed below), scattering off boundaries and that off defects. Each different physical process would depend differently on parameters like phonon energy and temperature, so at the early times, one method to avoid figuring out the exact expression is to approximate them with overall relaxation times. At the earliest time, all scatterings are conveniently included in a single parameter *tau*, and equation 2 becomes

$$-\vec{v}_\lambda \cdot \vec{\nabla} T \frac{\partial f^0_\lambda}{\partial T} = \frac{f_\lambda - f^0_\lambda}{\tau^0_\lambda} \tag{3}$$

where f^0_λ is $f_0(\omega_\lambda)$ for simplicity.

This is referred to as the relaxation time approximation (RTA). It not only triggers further development in modelling tranport experiments, but also serves as a reference point that people compare analysis and observations with. In 1959, Callaway distinguished the N process, which conserve phonon momentum, from the U process, where the phonon wavevectors add up to a reciprocal lattice vector, and the total τ^{-1} is written as sum of τ_U^-1 and τ_N^{-1} which have different ω and T dependence. More modifications have been proposed recently [[**Allen**]].

1.4 Linearized BTE

Nowadays, with advances in understanding the microscopic pictures of those scatterings and also computation power, a numerical approach towards solving BTE becomes favorable. The first step to simplify BTE is to linearize it. When $\vec{\nabla} T$ is small, one can taylor expand the phonon distribution around its equilibrium state as:

$$f_\lambda = f^0_\lambda + \left.\frac{\partial f_\lambda}{\partial T}\right|_{f_0} \nabla T + O(\nabla T^2) = -f^0_\lambda (1 + f^0_\lambda) \frac{\hbar \omega_\lambda}{k_B T^2} \phi_\lambda + O(\phi^2_\lambda) \tag{4}$$

and ϕ_λ is a small deviation. Inserting to equation 2, we get

$$\begin{aligned} -\vec{v_\lambda} \cdot \vec{\nabla} T \frac{\partial f^0_\lambda}{\partial T} = \frac{1}{N} \sum_{\lambda' \lambda''} \Big\{ & \Gamma^+_{\lambda \lambda' \lambda''} (\phi_\lambda + \frac{\omega_{\lambda'}}{\omega_\lambda} \phi'_\lambda - \frac{\omega_{\lambda''}}{\omega_\lambda} \phi''_\lambda) \\ & + \frac{1}{2} \Gamma^-_{\lambda \lambda' \lambda''} (\phi_\lambda - \frac{\omega_{\lambda'}}{\omega'_\lambda} \phi_{\lambda'} + \frac{\omega_{\lambda'}}{\omega''_\lambda} \phi_{\lambda''}) + \sum_{\lambda'} \Gamma_{\lambda \lambda'} \frac{\omega_{\lambda'}}{\omega_\lambda} \phi_{\lambda'} \Big\} \end{aligned} \tag{5}$$

Here, we are discretizing the Brilloin zone (BZ) into N total grid points. $\Gamma_{\lambda\lambda'}$ is the rate of scattering off isotopes and $\Gamma^\pm_{\lambda\lambda'\lambda''}$ are the rates of the three phonon scattering, where $\pm$ corresponds to adsorption and emission processes. The allowed groups of phonons involved are constrained by the conservation of energy and momentum, requiring that

$$\vec{q}_\lambda \pm \vec{q}_{\lambda'} = \vec{q}_{\lambda''} + \vec{G}, \quad \omega_\lambda \pm \omega_{\lambda'} = \omega_{\lambda''}$$

where $\vec{G}$ is either zero for N process or a reciprocal lattice vector for U processes.

Treating ϕ_λ as the leading linear term in ∇T, we can then insert $\phi_\lambda = -\vec{F}_\lambda \cdot \vec{\nabla} T$ into equation 5, resulting in a simplified set of linear equations:

$$\begin{aligned} \Big[-\vec{v}_\lambda \frac{\partial f^0_\lambda}{\partial T} + \frac{1}{N} \sum_{\lambda' \lambda''} \Big\{ & \Gamma^+_{\lambda \lambda' \lambda''} (\vec{F}_\lambda + \frac{\omega_{\lambda'}}{\omega_\lambda} \vec{F}_{\lambda'} - \frac{\omega_{\lambda''}}{\omega_\lambda} \vec{F}_{\lambda''}) \\ & + \frac{1}{2} \Gamma^-_{\lambda \lambda' \lambda''} (\vec{F}_\lambda - \frac{\omega_{\lambda'}}{\omega_\lambda} \vec{F}_{\lambda'} - \frac{\omega_{\lambda''}}{\omega_\lambda} \vec{F}_{\lambda''}) + \Gamma_{\lambda \lambda'} \frac{\omega_{\lambda'}}{\omega_\lambda} \vec{F}_{\lambda'} \Big\} \Big] \cdot \vec{\nabla} T = 0 \end{aligned} \tag{6}$$

Moving the first term to the right gives the familiar form

$$\mathbf{A} \cdot \vec{F} = \vec{b} \tag{7}$$

Finally, once we know $\vec{F}_\lambda$, we can sum up the modes and calculate thermal conductivity according to the Fourier law $\vec{J} = \kappa \cdot (-\vec{\nabla} T)$:

$$\kappa^{\alpha\beta} = \frac{1}{k_B T N V_{uc}} \sum_\lambda f_\lambda^0 (f_\lambda^0 + 1)(\hbar\omega_\lambda)^2 v_\lambda^\alpha F_\lambda^\beta \tag{8}$$

α and β are the real space Cartesian coordinates and V_{uc} is the volume of the unit cell.

2 Methodology

This project aims to solve equation 6 with simple iterative methods, and examines the thermal conductivity from the calculations. With abundant experimental data to compare with, and the strong motivation to achieve predictive power, a good numerical analysis is highly desirable. As mentioned before, there has been many progress in recent years, thanks to the development in calculating the transition rates Γ and phonon dispersion through *ab initio* methods. *Quantum Espresso* and *Phonopy* are two examples of the mature packages which have been widely used [[7]][[4]]. They can simulate phonon bands and atomic forces based on density functional theories together with numerical methods. Built upon that, Wu and others have published an integrated package that can calculate thermal conductivity directly, given certain material information [[8]]. This project is highly inspired by their papers and follows the general idea of the calculations, but tries to compare different numerical methods of the iterative steps, where originally the authors use a Jacobian method [[5][6]].

2.1 Iterative Methods

To start the iterations, it's natural to use the RTA value as an initial guess. The RTA results would be same as leaving out any detailed interactions between phonon modes, but just apply a general relaxation term instead. In other words, equation 6 can be reformulated into

$$\vec{F}_\lambda = \tau_\lambda^0 \left(\vec{v}_\lambda + d\vec{F}_\lambda\right) \tag{9}$$

where τ_λ^0 approximates the averaged scattering effects as

$$\frac{1}{\tau_\lambda^0} = \frac{1}{N}\Big(\sum_{\lambda'\lambda''}^{+} \Gamma^+_{\lambda\lambda'\lambda''} + \sum_{\lambda'\lambda''}^{-} \frac{1}{2}\Gamma^-_{\lambda\lambda'\lambda''} + \sum_{\lambda'} \Gamma_{\lambda\lambda'}\Big) \tag{10}$$

Hence setting $\vec{F}_\lambda = 0$ gives the RTA value. We can approach the solution through iterations by first writing equation 7 as

$$(\mathbf{I} - \mathbf{M}) \cdot \vec{F} = \vec{b}$$

and therefore

$$\tau_\lambda^0 \, d\vec{F}_\lambda = \mathbf{M} \cdot F$$

where we have

$$\begin{aligned} d\vec{F}_\lambda = \frac{1}{N}\sum_{\lambda'\lambda''}^{+} \Gamma^+_{\lambda\lambda'\lambda''}\Big(\frac{\omega_{\lambda'}}{\omega_\lambda}\vec{F}_{\lambda'} - \frac{\omega_{\lambda''}}{\omega_\lambda}\vec{F}_{\lambda''}\Big) \\ + \frac{1}{N}\sum_{\lambda'\lambda''}^{-} \frac{1}{2}\Gamma^-_{\lambda\lambda'\lambda''}\Big(\frac{\omega_{\lambda'}}{\omega_\lambda}\vec{F}_{\lambda'} + \frac{\omega_{\lambda''}}{\omega_\lambda}\vec{F}_{\lambda''}\Big) + \frac{1}{N}\sum_{\lambda'} \Gamma_{\lambda\lambda'}\frac{\omega_{\lambda'}}{\omega_\lambda}\vec{F}_{\lambda'} \end{aligned} \tag{11}$$

The original package uses the Jacobian method, hence the iteration step in explicit form is

$$(\vec{F}_\lambda)_i^{n+1} = (\vec{F})_i^0 + \sum_{j=1, j\neq i}^{N} M_{i,j}\,(d\vec{F_\lambda})_j^n \qquad \text{Jacobian} \tag{12}$$

On the other hand, we can also employ Gauss-Seidel method, which looks like

$$(\vec{F}_\lambda)_i^{n+1} = (\vec{F})_i^0 + \sum_{j=1}^{i-1} M_{i,j} \, (d\vec{F_\lambda})_j^{n+1} + \sum_{j=i+1}^{N} M_{i,j} \, (d\vec{F_\lambda})_j^n \qquad \text{Gauss-Seidel} \qquad (13)$$

and also sucessive over-relaxation (SOR) with a relaxation parameter ω (not to confuse with the phonon frequency)

$$(\vec{F}_\lambda)_i^{n+1} = (\vec{F})_i^0 + \omega \left(\sum_{j=1}^{i-1} M_{i,j} \, (d\vec{F_\lambda})_j^{n+1} + \sum_{j=i+1}^{N} M_{i,j} \, (d\vec{F_\lambda})_j^n \right) \qquad \text{SOR} \qquad (14)$$

2.2 Inputs and Outputs

The inputs to the calculations discussed here include scattering rates, phonon bands, and group velocities. Symmetry of the crystal is not absolutely necessary, but is crucial in minimize the computing cost. Determining the scattering rates have been the limiting step in numerically solving BTE, and indeed the *ab initio* calculations are quite involved and deserve its own discussion elsewhere. For common materials, one can usually either get the information from publicly available software like the ones mentioned above, or least approximate it based on the results from those resources. The package referred to in this project, *ShengBTE*, also needs to take the 2nd order and 3rd order atomic force constants as inputs, which describe the interaction strengths between 2 and 3 atoms. These can be generated by either *Phonopy* or *Quantum Espresso* with their built-in DFT calculations and finite difference approximations, together with other information like phonon dispersion. Based on the force constants, *ShengBTE* calculates the scattering rates. It takes into account the energy conservation by approximating available scattering range with a Gaussian function with a locally adaptive width. These are both numerical steps that are worth explored further, but left out here due to time constraints. Here, the project takes the scattering rates and phonon dispersion from examples provided online. Yet in principle, one can simulate the thermal conductivity of any materials just with limited information and DFT analysis software.

3 Calculations and Results

This paragraph summarizes the structure of the coding set up. It can be separated into three major parts: importing, numerical calculations, and testing and plotting. The middle part can be further divided into five steps: 1) calculating RTA values as the initial guesses, 2) locating the symmetry allowed groups for absorption and emission processes, 3) updating $d\vec{F}_\lambda$ for one phonon mode given its wavevector and phonon branch, 4) updating all phonon modes according to the specific algorithm, and finally 5) iterating till desired performance.

3.1 Discretization and Computation Cost

While discretizing the BZ into $N = N_1 \times N_2 \times N_3$ grids (which is basically equivalent to a Fourier analysis of the lattice), it's important to keep in mind about the crystal symmetry and the computation cost, especially given the presence of three phonon processes. Say n is the number of points along one crystal axis. Without any symmetry analysis and allows every scattering to happen, there are n^3 modes in total. For each point, there are $(n^3)^2$ terms for each processes of absorption and emission, and it mounts up to $2n^6 + n^3$ steps when adding the isotopic effect. Hence for one iteration, there are roughly $2n^9 + n^3$ steps, so for m iterations, the calculation scales as $O(m\, n^9)$, not to mention there are usually multiple phonon branches at each point. Symmetry hugely reduces this number. In fact, for the case of a $12 \times 12 \times 12$ grids of InAs, it is cut down by a power of 2: there are only 72 irreducible points in total after symmetry reduction, each with 6 bands. It not only minimizes number of $d\vec{F}_\lambda$ to update, but also cuts down the three-process terms $\Gamma^{\pm}_{\lambda\lambda'\lambda''}$ impressively. Within this irreducible set, there are usually same size of a group for each point that are allowed by momentum conservation. Hence in general, the expense is scaled down to just $O(m\, n^{3/2})$, rendering it possible to reach a fair enough performance even on personal laptops. However, to harvest the most from the symmetry analysis,

it's noteworthy to select grid numbers that are consistent with the crystal symmetry. For example, selecting $N_1 = N_2 = N_3$ for a cubic structure leads to the most reduction.

3.2 Conservation

As mentioned above, the conservation of quasi-momentum is important not only for reflecting the physics, but also for minimizing the computation cost. In the setup here, it is a pre-processing step given the list of irreducible wavevectors, and it is done before updating any $d\vec{F}_\lambda$. They are found out by checking the sum and difference of the wavevectors one by one. Of course, changing the grid size would change the number of this minimal set, and hence also the groups allowed by conservation. Let p_0, p_1, and p_2 be the phonons involved in one scattering. Then given a specific p_0, a dictionary is generated with (p_1, p_2) as key-value pairs. For each set of irreducible grids, there are two overall dictionaries where each p_0 is the key, and they correspond to absorption and emission processes.

3.3 Iteration

The first step of the iterations is to find out the initial value $d\vec{F}^0_\lambda = \tau^0_\lambda \vec{v}_\lambda$. Here for simplicity, the following part and codes only concerns the longitudinal thermal conductivity along x-axis, namely the entry κ_{xx} of the tensor, but the mechanism for other components would be exactly the same (most of them are already the same values by symmetry). The method `update_df_pb` (which can be found on github) calculates dF^x_λ at a specific mode. The three different methods presented below all call on this common method, but prompt it with sets of dF^x at different iterations steps. Below is the code snippet of iterating dF^x_λ via the Jacobian method.

```
    # iterate df once, output n*1 vector
    def update_df_all_jac(fin,omegain,dict_pin,dict_min,tau0in):
        df_all = np.zeros(fin.size)
        for i in range(fin.size):
            if omegain[i%Nq,i//Nq] != 0:
                df_all[i] = update_df_pb(fin,i,omegain,dict_pin,dict_min,tau0in)
        return df_all.reshape(-1,1)

    # iterate k multiple times
    def iterate_k_jac(nnITER,tt,Ntot,Vin,f0in,n0in,omegain,vxin,degeneracy,dict_pin,
    dict_min,tau0in):

        fold = f0in[:]
        flist = [fold]
        dflist = [[0]*f0in.size]
        k0 = calc_k(f0in,tt,Ntot,Vin,n0in,omegain,vxin,degeneracy)
        klist = [k0]
        for _ in range(nnITER):
            df = update_df_all_jac(fold,omegain,dict_pin,dict_min,tau0in)
            #print(np.max(abs(df)))
            dflist.append(df)
            fn = f0in + df.reshape(-1,1)
            flist.append(fn)
            klist.append(calc_k(fn,tt,Ntot,Vin,n0in,omegain,vxin,degeneracy))
            fold = fn

        return flist,klist,dflist
```

The code that implements the Gauss-Seidel method to calculate the full $d\vec{F}_\lambda$ (except for the exact degeneracies) is shown below. The method for its corresponding step to calculate the thermal conductivity is pretty similar to the Jacobian case, and can be found in on the github.

```
    def update_df_all_gs(fin,omegain,dict_pin,dict_min,tau0in):
        fold_step = np.copy(fin)
        length = fold_step.size
        df_all = np.zeros(length)
        df_all_i=0

```

```
        for i in range(length):
            if omegain[i%Nq][i//Nq] != 0:
                df_all_i = update_df_pb(fold_step,i,omegain,dict_pin,dict_min,tau0in)
                df_all[i] = df_all_i
            fold_step[i] = fold_step[i]+df_all_i

        return df_all.reshape(-1,1)
```

The snippet below shows the method implementing SOR. Again, calculating κ is pretty similar to the previous ones. In fact, one of the next improvements would be to combine them in a general method that takes the specific algorithms as an input parameter.

```
    def iterate_k_sor(fac,nnITER,tt,Ntot,Vin,f0in,n0in,omegain,vxin,degeneracy,
    dict_pin,dict_min,tau0in):

    fold = np.copy(f0in)
    flist = [fold]
    dflist = [[0]*fold.size]
    k0 = calc_k(f0in,tt,Ntot,Vin,n0in,omegain,vxin,degeneracy)
    klist = [k0]
    #print(klist)
    for _ in range(nnITER):
        df = update_df_all_gs(fold,omegain,dict_pin,dict_min,tau0in)*fac
        #print(np.max(abs(df)))
        dflist.append(df)
        fn = f0in + df.reshape(-1,1)
        flist.append(fn)
        klist.append(calc_k(fn,tt,Ntot,Vin,n0in,omegain,vxin,degeneracy))
        #print(klist)
        fold = fn

    return flist,klist,dflist
```

3.4 Results

Here, a $4 \times 4 \times 4$ grid set is adapted to calculate the case of InAs, which has a zinc-blende structure. The 64 points are reduced to 8 distinguished point within the first BZ, and at each point 6 phonon branches are considered. The results are quite peculiar and presented in Figure 2. For reference, the same input numbers are run through *ShengBTE* and the resultant temperature dependence of $\kappa_x x$ is plotted below in Figure 1. The first thing to note, unfortunately, is that there seems to be a factor of 10 difference between the iterative results and the reference: 4.183 versus 40.24 at 50K and 0.64 versus 6.5 at 300K. This is checked at several temperatures, and it's present in the RTA values. It's still uncertain that whether it comes from the algorithms or bugs hidden in the codes. If it's the latter case, because RTA numbers should be unaffected by the iterations, any typo in the codes should be among the pre-processing steps. Calculation of τ_λ^0 is the most likely source, but it's pretty short and readers are welcome to take a look together.

The next interesting observation is the unexpected behaviors of the iterative methods. Firstly, the convergence is too fast to notice a clear trend for all three methods. However, this is also something noticed by the package contributors, that for materials with dominant U scatterings like InAs, the numerical calculations do not differ from the RTA a lot. As demonstrated in Figure 1, the curves almost overlap for both choices of grid sizes. Since change in dF_λ^x is around 10^{-9} 10^{-12}, it's hard to quantitatively measure how fast the convergence is. Yet it's pretty obvious from Figure 2 that all three methods converge too fast enough to note any visible change after 2 to 3 times. From the plot, Jacobian and Gauss-Seidel seem to have a larger swing than SOR at the initial steps, which is likely due to the relaxation nature of SOR algorithm.

It's also quite unexpected that the SOR method converge to a very different result compared to the other two. It seems that after the initial steps, the iteration loses its power to change from previous values, and hence the convergent result is highly determined by the effects at the beginning. One possible explanation is that the grid size taken is too small to see enough interactions to take place. More runs at different temperatures and different grid sizes are needed to draw further conclusions.

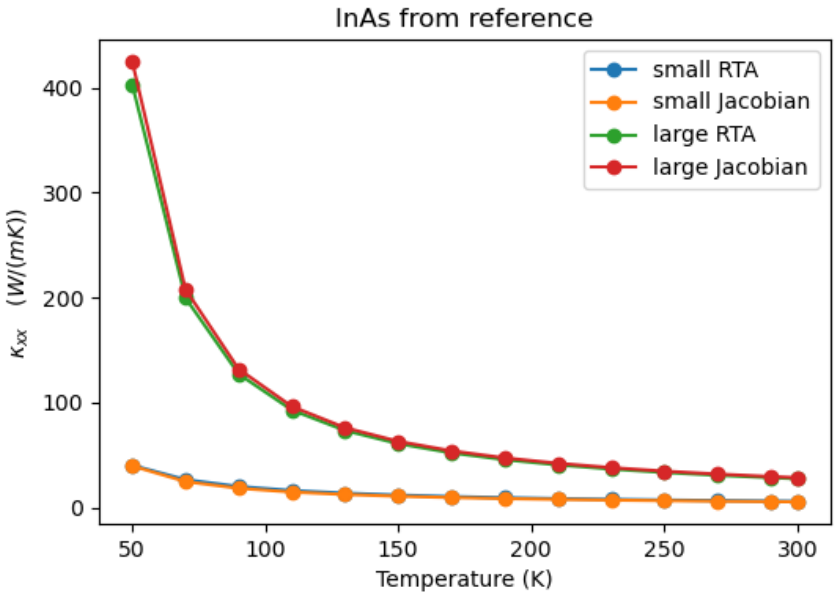

Figure 1: Reference data obained by running through external package [8]. Blue and yellow curves are calculations based on a smaller grid size $4 \times 4 \times 4$. Red and green curves are those on a larger grid size $12 \times 12 \times 12$.

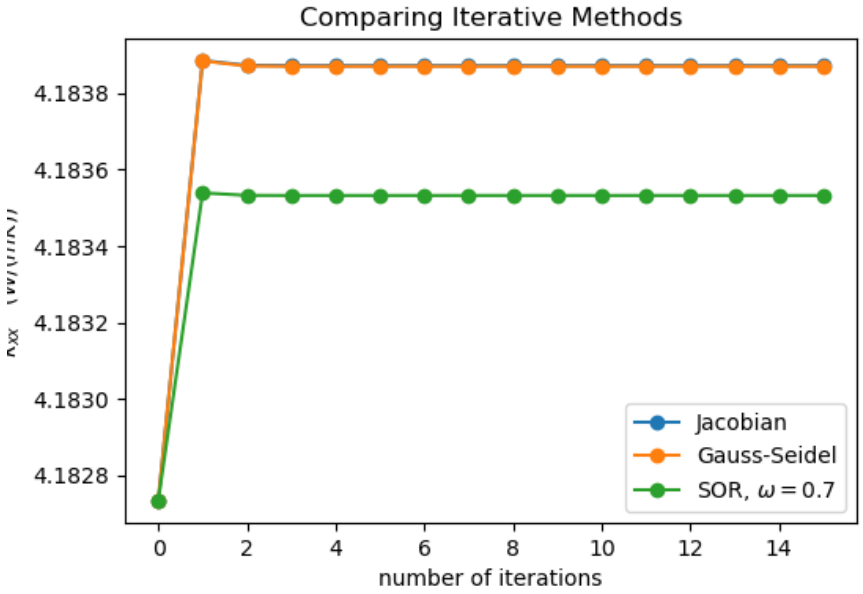

Figure 2: Data calculated on the same $4 \times 4 \times 4$ grid for InAs. The blue and orange plots the data obtained with Jacobian and Gauss-Seidel methods, respecively, and overlap almost completely. The green plot shows the SOR method, with $\omega = 0.7$.

4 Conclusion and Outlook

To conclude, this project takes the iterative approach to solve linearized phonon BTE numerically. Specifically, it compares among Jacobian, Gauss-Seidel, and SOR methods. Various scattering mechanisms (including N process, U process, and isotopic scattering) are taken care of through different transition rates, and can be generated by publicly available packages. The RTA treatment, which averages all scattering effects with a tunable parameter, serves as both a reference and the initial guess. Symmetry and conservation laws are crucial in cutting down the computation expense, and they in principle can reduce the scaling from $O(m\,n^9)$ to roughly $O(m\,n^{3/2})$. A simple case of InAs on a $4 \times 4 \times 4$ is presented here, where all three methods converge within 2 to 3 steps. While Jacobian and Gauss-Seidel demonstrate almost same performances, SOR shows a less violent change and converges to a value that differs less from the initial guess. There're many aspects that are worth further studying, including behaviors on a larger grid size, cases in other materials where RTA deviate a lot from experiment values, and if the performances would vary at more exotic crystal symmetries.

References

[1] JAN Bruin et al. "Robustness of the thermal Hall effect close to half-quantization in α-RuCl3". In: *Nature Physics* 18.4 (2022), pp. 401–405.

[2] Joseph Callaway. "Model for Lattice Thermal Conductivity at Low Temperatures". In: *Phys. Rev.* 113 (4 Feb. 1959), pp. 1046–1051. DOI: 10.1103/PhysRev.113.1046. URL: https://link.aps.org/doi/10.1103/PhysRev.113.1046.

[3] Peter Czajka et al. "Oscillations of the thermal conductivity in the spin-liquid state of α-RuCl3". In: *Nature Physics* 17.8 (2021), pp. 915–919.

[4] Quantum Espressor. URL: https://www.quantum-espresso.org/.

[5] Wu Li et al. "Thermal conductivity of bulk and nanowire $Mg_2Si_xSn_{1-x}$ alloys from first principles". In: *Phys. Rev. B* 86 (17 Nov. 2012), p. 174307. DOI: 10.1103/PhysRevB.86.174307. URL: https://link.aps.org/doi/10.1103/PhysRevB.86.174307.

[6] Wu Li et al. "Thermal conductivity of diamond nanowires from first principles". In: *Phys. Rev. B* 85 (19 May 2012), p. 195436. DOI: 10.1103/PhysRevB.85.195436. URL: https://link.aps.org/doi/10.1103/PhysRevB.85.195436.

[7] Phonopy. URL: https://phonopy.github.io/phonopy/index.html.

[8] ShengBTE. URL: https://bitbucket.org/sousaw/shengbte/src/master/.

[9] T. Yokoi et al. "Half-integer quantized anomalous thermal Hall effect in the Kitaev material candidate α-RuCl¡sub¿3¡/sub¿". In: *Science* 373.6554 (2021), pp. 568–572. DOI: 10.1126/science.aay5551. eprint: https://www.science.org/doi/pdf/10.1126/science.aay5551. URL: https://www.science.org/doi/abs/10.1126/science.aay5551.